

# Pre-symptomatic Transmission in the Evolution of the COVID-19 Pandemic

Liang Tian<sup>1,2,\*</sup>, Xuefei Li<sup>1,3,\*</sup>, Fei Qi<sup>1,3</sup>, Qian-Yuan Tang<sup>1,4</sup>, Viola Tang<sup>1,5</sup>, Jiang Liu<sup>1,6</sup>, Xingye Cheng<sup>1,2</sup>, Xuanxuan Li<sup>1,7,8</sup>, Yingchen Shi<sup>1,7,8</sup>, Haiguang Liu<sup>1,8,9</sup>, Lei-Han Tang<sup>1,2,8,#</sup>

\*Contributed equally

Affiliations:

<sup>1</sup>COVID-19 Modelling Group, Hong Kong Baptist University, Kowloon, Hong Kong SAR, China

<sup>2</sup>Department of Physics and Institute of Computational and Theoretical Studies, Hong Kong Baptist University, Kowloon, Hong Kong SAR, China

<sup>3</sup>CAS Key Laboratory of Quantitative Engineering Biology, Shenzhen Institute of Synthetic Biology, Shenzhen Institutes of Advanced Technology, Shenzhen 518055, China

<sup>4</sup>Center for Complex Systems Biology, Universal Biology Institute, University of Tokyo, 113-0033 Tokyo, Japan

<sup>5</sup>Department of Information Systems, Business Statistics and Operations Management, Hong Kong University of Science and Technology, Hong Kong SAR, China

<sup>6</sup>Scarsdale, NY 10683, USA

<sup>7</sup>Department of Engineering Physics, Tsinghua University, Haidian, Beijing 100084, China

<sup>8</sup>Complex Systems Division, Beijing Computational Science Research Center, Haidian, Beijing 100193, China

<sup>9</sup>Physics Department, Beijing Normal University, Haidian, Beijing 100875, China

#Correspondence: [lhtang@hkbu.edu.hk](mailto:lhtang@hkbu.edu.hk), Lei-Han Tang, Department of Physics, Hong Kong Baptist University, Hong Kong SAR, China

## Abstract:

The Coronavirus Disease 2019 (COVID-19), has infected more than 170,000 people globally and resulted in over 6,000 deaths over a three-month period <sup>1,2</sup>. Contrary to mainstream views, there is growing literature on pre-symptomatic and asymptomatic individuals contributing significantly to the disease outbreak. Several recent studies on serial infection yielded a mean interval of around 4 days, shorter than the mean symptom onset time of 5-7 days, and negative serial interval in more than 10% of the cases <sup>3-5</sup>. These observations highlight the urgent need to quantify the pre-symptomatic transmission for adequate global response <sup>6,7</sup>. In this paper, we develop an epidemic model driven by pre-symptomatic transmission. Within the model construct, the infectiousness of a viral carrier on a given day is identified with their symptom onset probability, which we characterise through extensive studies of the clinical literature. The well-known Lotka–Euler estimating equation can then be invoked to relate the daily growth rate  $\lambda$  of the epidemic with the basic reproduction number  $R_0$ . We applied the disease spreading model to epidemic development in affected provinces across China following the Wuhan lockdown on January 23, 2020. The remarkable three-phase universal pattern can be well-captured by the model. Despite its simplicity, the model allows synthesis of data from

diverse sources to form a quantitative understanding of key mechanisms that drive or contain the disease spreading, and to make informed decisions to bring the pandemic under control.

**Keywords:** COVID-19, Coronavirus, Quarantine, Disease transmission model, Pre-Symptomatic, Asymptomatic, Epidemic, Pandemic

## Introduction

The Coronavirus Disease 2019 (COVID-19) is a new contagious disease caused by the novel coronavirus (SARS-CoV-2)<sup>8</sup>, which belongs to the genera of *betacoronavirus*, the same as the coronavirus that caused the SARS epidemic between 2002 and 2003<sup>9</sup>. COVID-19 has spread to more than 140 countries, infecting over 170,000 people and claiming over 6,000 lives. As a result, the outbreak has been declared a pandemic and a public health emergency of international concern<sup>1</sup>.

Various measures to contain COVID-19 have been taken by governments around the world. A regional lockdown, such as the one enforced on the city of Wuhan on January 23, 2020, is one extreme implementation. Subsequently, similar quarantine measures have been implemented in other parts of mainland China. As a result, the majority of infected cases were confined to a region surrounding Wuhan, and other regions experienced a much smaller scale of infection. In some countries, such stringent policies may not be practically feasible nor supported by the public. The question is how stringent the isolation measures should be to contain the epidemic, while taking into consideration their implementation and economic costs, especially for larger populations. To answer this question effectively, we must account for the nature of the disease, including its natural progression, reproductive ratio and transmission rate.

COVID-19 has a high infection rate, exhibited as the exponential growth at the early transmission stage before government intervention takes place<sup>10</sup>. The contagious characteristics of COVID-19 before its major symptom onset makes it more challenging to track and contain. In the case of pre-symptomatic transmission, epidemiology studies suggested that more stringent quarantine measures are required to contain the virus<sup>5,11</sup>. Due to its long incubation time of 5 to 7 days, pre-symptomatic or asymptomatic carriers may constitute a significant proportion of the overall infected population, 51% in the case of the Diamond Princess cruise ship based on data from February 20, 2020, when passengers began to disembark<sup>12</sup>, or a lower rate of 17.9 % estimated by Mizumoto et al.<sup>13</sup>. A number of studies suggested that this group of viral carriers could contribute significantly to the spread of the virus<sup>3,4,14-17</sup>. Mathematical modeling of the COVID-19 outbreak can be used to assess its progression at the population level and this paper provides the first explicit model for the evolution of COVID-19 driven by the pre-symptomatic population.

In epidemiological studies, accurate estimation of the basic reproduction number,  $R_0$ , is important for predicting the spread of a disease. For COVID-19, several methods have been applied to estimate  $R_0$  such as analyzing the real-time cumulative cases by way of various statistical analyses<sup>18-22</sup>, fitting SEIR-type model parameters to the data<sup>23</sup>, and fitting logistic growth model parameters to the data<sup>24</sup>. The  $R_0$  values reported in these studies are in the range of 2.1 to 6.4, with a mean value of 3.5.

Additionally, the growth and decay rates,  $\lambda$ , of confirmed cases serve as a direct way to project short-term epidemic development. Previously, Wallinga and Lipsitch <sup>25</sup> demonstrated that given the generation interval distribution,  $\lambda$  and  $R_0$  can be connected. However, the generation time distribution in a given community requires unbiased sampling of a large number of cases where both the infector and infected need to be monitored throughout their disease development, which is generally challenging. Therefore, an alternative framework based on a more easily accessible data source, e.g., the distribution of incubation period or serial interval, can be immediately helpful for this purpose.

As the basic physiological and clinical progression of the COVID-19 disease is being understood, hospitals and public health authorities have taken aggressive measures to eradicate symptomatic transmission. Consequently, the pre-symptomatic transmission is attracting much greater attention. In existing studies on COVID-19, a few mathematical modeling efforts considered the infections from the virus carriers during their incubation periods, such as the stochastic transmission model with asymptomatic transmission<sup>26</sup> and SEIR-type model with an infectious latent population<sup>27,28</sup>. Their results, often in numerical form, yield valuable insights on how different model parameters and control measures affect the growth of the infected population.

An alternative modeling strategy was proposed by Fraser et al. <sup>29,30</sup> to identify optimal control measures to contain a disease outbreak given its  $R_0$  and the pre-symptomatic infection fraction  $\theta$ . Despite the simple construct of their approach, they were able to predict that influenza, which can transmit before the symptom onset ( $30\% < \theta < 50\%$ ), would be very difficult to control even with 90% quarantining and contact tracing because of the high level of pre-symptomatic transmission. On the other hand, a SARS outbreak can be controlled by isolating symptomatic patients ( $\theta < 11\%$ ). The work by Fraser et al. demonstrated that optimal control measures require a detailed understanding of the nature of the disease.

In this paper, we develop the modeling strategy by Fraser et al. to a form that facilitates the incorporation of accessible data on disease progression and transmission pattern. Upon exposure to sufficient viral load, there is an incubation period when the individual is not infectious. Transmission takes place in the time window from the end of the first period to symptom onset, and could continue after symptoms develop. We quantify the contribution of these processes to the growth of the pre-symptomatic population through an integro-differential equation. It turns out that the kernel function that describes the delay associated with the initial viral incubation can be expressed in terms of the distribution function for the whole period before symptom onset. As the latter can be measured directly in clinical studies, we have on hand the ingredients for a quantitative model which, when combined with knowledge about social contacts, yields a realistic description of epidemic spread in a given community.

The Wuhan lockdown marks a critical time point in the COVID-19 epidemic development in China. Based on data obtained from the JHU CSSE repository <sup>2</sup>, the number of newly confirmed cases continued to grow at approximately 0.3 per day across the country after the lockdown. In our model, this growth rate is driven by imported cases from the epidemic center of Wuhan. Upon shutting down the imported cases from Wuhan, the epidemics in other provinces entered a crossover phase lasting two to three weeks under stringent tracking, isolation and quarantine measures. By examining various scenarios on how the model parameter  $R_0$  changes with time in connection with data from online archives and extensive media reports, we bring an interpretation of the crossover phase. Finally, once the transmission is completely shut off, the statistics of the onset time, which we compile from previous case

studies on SARS-CoV-2 infection<sup>15,31,32</sup>, yields an upper bound on the final decay which is realized by the daily confirmed infections in China.

Although the extent of pre-symptomatic transmission since the Wuhan lockdown remains to be quantified, the agreement between our model predictions and data on epidemic development across China gives credence to the modelling strategy. In the next sections we outline the key aspects of the model and discuss our findings and interpretations. The results highlight the critical importance of quickly implementing proper control and treatment to both the symptomatic and pre-symptomatic carriers in containing the outbreak, which is a valuable outcome for policy-makers around the world to consider.

## The Model

### Model structure and the evolution equation

We adapted the general mathematical modeling framework for epidemic spreading described by Fraser et al.<sup>29</sup> to an explicit form that enables direct determination of model parameters from clinical case studies. The basic structure of the model is shown in Fig. 1.

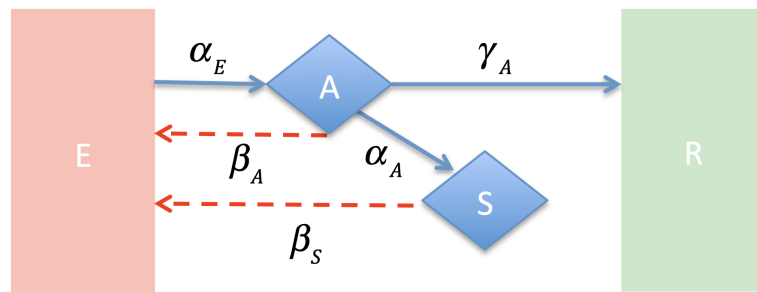


**Figure 1. Diagram of the model for studying COVID-19 epidemic development.**

An infected individual is classified into one of four states: exposed but not yet infectious ( $E$ ), asymptomatic and infectious ( $A$ ), symptomatic ( $S$ ), and inactive ( $R$ ). Starting from an individual in state  $E$ , the transition to state  $A$  takes place at a rate  $\alpha_E$ . Once in state  $A$ , the individual develops symptoms at a rate  $\alpha_A$ , or turns into  $R$  at a rate  $\gamma_A$ . The rate of disease transmission in state  $A$  and  $S$  are given by  $\beta_A$  and  $\beta_S$ , respectively. To better account for observational data, we take  $\alpha_E$  and  $\beta_S$  to be functions of the time an individual is in state  $E$  (exposed) and state  $S$  since their respective onsets. The other parameters are treated as constants for a given community. We note in passing that the ratio  $\gamma_A/(\alpha_A + \gamma_A)$  gives the fraction of infected individuals whose contribution to disease transmission is limited by the exit mechanism, due to either natural recovery or removal procedures.

We use the same symbol as the state itself to denote the respective population size. Focusing on the population in state  $A$ , its dynamics are driven by the two feedback processes indicated by the red arrows. Given a history of  $A$ , we express its rate of increase as,

$$\dot{A} = -(\alpha_A + \gamma_A)A + \int_{-\infty}^t K(t - t_1)A(t_1)dt_1 \quad (1)$$

where the kernel function is given by

$$K(t) = \beta_A \alpha_E(t) q_E(t) + \alpha_A \int_0^t \alpha_E(t - t_1) q_E(t - t_1) \beta_S(t_1) dt_1$$

Here,  $q_E(t) = e^{-\int_0^t \alpha_E(t_1) dt_1}$  is the probability that an individual infected at  $t = 0$  remains in state  $E$  after time  $t$ . Equation (1) is our basic dynamical equation for epidemic development without flux of imported cases. The mathematics behind this type of epidemic spreading models has been extensively studied in the literature<sup>29,33</sup>.

When infection by a symptomatic individual takes place only during the initial period of symptom onset, we may approximate the transmission rate  $\beta_S(t) \approx \tilde{\beta}_S \delta(t)$ , where  $\delta(t)$  is the Dirac delta-function. The kernel function in this is reduced to

$$K(t) = \beta_{\text{eff}} \alpha_E(t) q_E(t),$$

where  $\beta_{\text{eff}} = \beta_A + \alpha_A \tilde{\beta}_S$  is an effective transmission rate, with contributions from symptomatic carriers. We shall consider this simpler model in the rest of the Main Text.

## Symptom onset time and the reproduction rate

Directly observable from case studies is the time interval between exposure and symptom onset  $\tau_O = \tau_E + \tau_A$ , whose distribution  $p_O(t)$  can be determined from the transition rates  $\alpha_E(t)$  and  $\alpha_A$  associated with disease progression. In the Supplementary Information, we present a derivation that yields the key result of this work, i.e., the distribution  $p_O(t)$  and the reproduction rate  $r(t)$  at time  $t$  from infection are related by,

$$r(t) = \left( \frac{\beta_A}{\alpha_A} + \tilde{\beta}_S \right) \left[ p_O(t) - \gamma_A \int_0^t dt_1 p_O(t_1) e^{-(\alpha_A + \gamma_A)(t-t_1)} \right]. \quad (2)$$

The removal rate  $\gamma_A$  reduces  $r(t)$  by terminating pre-symptomatic and ensuing transmission. Integrating the expression, we obtain the basic reproduction number

$$R_0 = \frac{\beta_{\text{eff}}}{\alpha_A + \gamma_A} \quad (3)$$

which gives the average number of second-generation individuals infected by a viral carrier during their lifetime. It is clear from Eq. (3) that  $R_0$  can be reduced by either reducing the transmission rate  $\beta_{\text{eff}}$  through social distancing or by increasing the removal rate  $\gamma_A$  through aggressive tracking and isolation of asymptomatic yet infectious individuals.

In terms of  $p_O(t)$ , we may express the kernel function as,

$$K(t) = \frac{\beta_{\text{eff}}}{\alpha_A} e^{-\alpha_A t} \frac{d}{dt} [e^{\alpha_A t} p_O(t)]. \quad (4)$$

This expression for the kernel function enables the prediction of the population size of asymptomatic infectors from clinical observations of symptom onset time.

With the help of Eq. (2), the well-known Lotka–Euler estimating equation<sup>25</sup> that relates  $R_0$  to the epidemic growth rate  $\lambda$  then takes the form,

$$R_0 = \frac{1}{\tilde{p}_0(\lambda)} \frac{\alpha_A}{\alpha_A + \gamma_A} \left( 1 + \frac{\gamma_A}{\alpha_A + \lambda} \right). \quad (5)$$

Below we present an explicit form of the relation by combining data from three separate studies where the statistics of the symptom onset time were collected.

## Results

### COVID-19 transmission patterns and universal parameters

From the time-series data of daily confirmed cases of COVID-19 obtained from the Johns Hopkins CSSE Repository<sup>2</sup>, we identify three universal phases of COVID-19 epidemic development from different places in China following the Wuhan lockdown on January 23, 2020. In the first week after the lockdown, the number of newly confirmed cases continued to grow at approximately 0.3 per day. This was followed by a crossover phase that lasted two to three weeks, during which provincial and local governments took stringent tracking, isolation and quarantine measures. In this phase, the growth rate slowed down and eventually turned negative upon reaching the much-desired inflection point. In the phase of final descent, the reduction of daily confirmed cases again took a universal form of exponential decay at a rate of 0.32 per day, i.e., a tenfold reduction in the number of newly confirmed cases per week (Fig. 2a).

In Hubei province, where the outbreak originated, the epidemics of COVID-19 showed a similar pattern (Fig. 2b). The number of daily confirmed cases followed an exponential growth at a similar rate to other provinces during the first one to two weeks after the lockdown. However, the crossover phase lasted for two more weeks compared to other provinces. Based on media reports, the much more elevated scale of the epidemic overwhelmed the local public health and disease control capabilities, suggesting a reduced but finite communal transmission that still existed. Starting from about March 3, 2020, the epidemic entered the final descent phase, in which the rate of decrease in the number of newly confirmed cases began to conform to and finally reached the value seen in the rest of the country.

While the outbreak is subsiding in China, exponential growth with a daily growth rate of around 0.3 is seen in the latest epidemic data from a number of countries around the world (Fig. 2c). In the past few days, data for the newly confirmed cases in Iran and South Korea have started to exhibit the type of turn-around seen in the crossover phase in China in February.

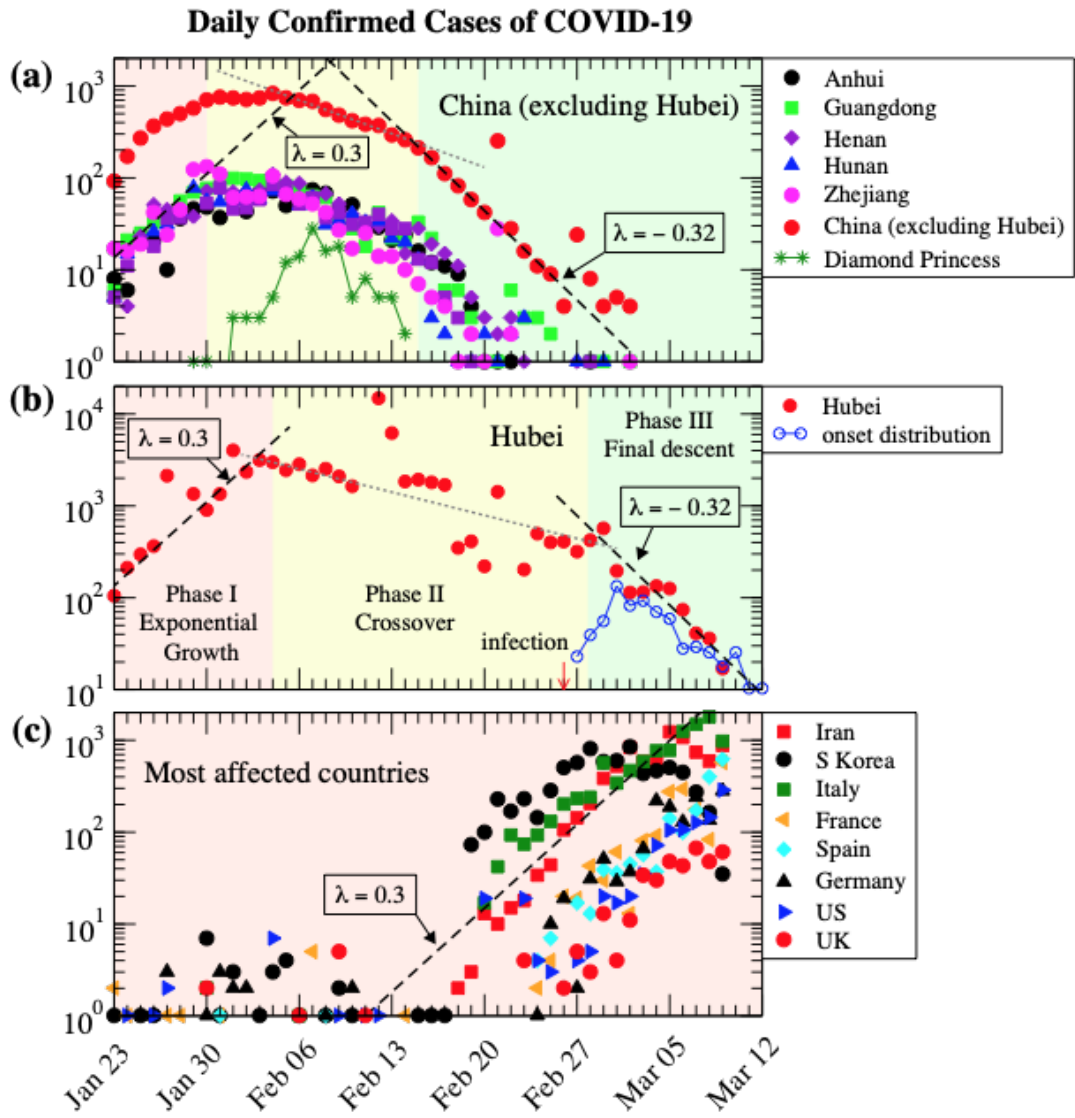


**Figure 2. The universal pattern of the COVID-19 epidemic development.** New daily confirmed cases in China and other affected countries since the Wuhan lockdown on January 23, 2020. **a.** China (excluding Hubei province). The epidemic development falls into three distinct phases: exponential growth phase (red area), crossover phase (yellow area), and final descent phase (green area). In the exponential growth phase, the number of newly confirmed cases grows at a daily rate  $\lambda$  of around 0.3 (left dashed line). In the crossover phase, the growth slows down and the number of daily confirmed cases begins to decrease after the inflection point (middle dotted line). In the final descent phase, the containment of COVID-19 follows a universal exponential decay at a daily rate  $\lambda = -0.32$  (right dashed line). Data for the Diamond Princess cruise ship is also shown for comparison. **b.** Hubei province. The epidemic development follows the same pattern as the rest of China. The distribution of symptom onset time (shifted) is shown for comparison. **c.** Other most affected countries. The epidemic progress for most of these countries is still in the exponential growth phase (red area) with a daily rate  $\lambda$  of around 0.3 (dashed line).

## Compilation of symptom onset data

### Symptom onset time distribution and the $R_0 - \lambda$ curve

The incubation periods of individual patients before symptom onset were summarized in 3 preprints: 39 cases collected from Shanghai by Lu et al.<sup>31</sup>, 54 cases collected by Men et al.<sup>32</sup>, and 105 cases collected by Xia et al.<sup>15</sup>. In total, we examined 198 cases with their incubation periods. For cases when the initial contact can only be assigned to a time interval spanning more than one day, we simply assume equal probability for each day inside the interval. We then include all case counts to construct the histogram of symptom onset time, rendering the result shown in Fig. 3a. The mean onset time is 5.5 days, with a standard deviation of 3.1 days. The tail of the distribution can be well-fitted to an exponential decay function with a slope of  $-0.32$ , in remarkable agreement with the final decline of the epidemic in affected provinces across China.

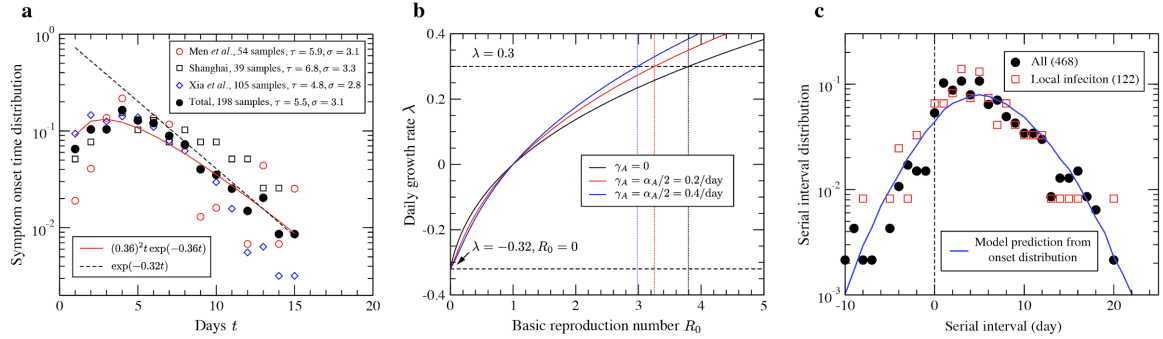


**Figure 3. Statistics of the incubation period before symptom onset and ensuing model predictions.** From the data of the incubation periods, our model can provide a quantitative relationship between  $\lambda$  and  $R_0$ , as well as the serial interval distribution. **a.** Probability of an infector to develop symptoms on the  $t$ -th day after infection. 3 data sets from previous studies are shown (red circles<sup>32</sup>, black squares<sup>31</sup>, and blue diamonds<sup>15</sup>). The mean values and standard deviations are given in the legend. The distribution by summing all 3 data sets is shown in black dots. Red solid and black dashed lines give reference functions shown in the legend. **b.** The relationship between  $\lambda$  and  $R_0$  for three different sets of model parameters. At  $\gamma_A = 0$ , the curve (black) is obtained directly from the Laplace transform of the data (black dots in **a**). Removal of the pre-symptomatic viral carriers at a rate  $\gamma_A$  makes the curve steeper. For growth rate  $\lambda = 0.3$  estimated in our analysis,  $R_0$  is estimated to be around 3, 3.2 or 3.8 with different values of  $\gamma_A$  (blue, red and black lines) shown in the legend. **c.** Predicted serial interval distribution vs. real data. The data collected by Du et al.<sup>4</sup> on the serial interval distribution is shown in black dots (all 468 pairs) and red squares (122 local infections). The blue line is our model prediction using the data for the incubation period as input (black dots in **a**).

We computed the Laplace transform of the symptom onset time distribution to determine the function  $\lambda(R_0)$  according to Eq. (5). The result is shown by the black line in Fig. 3b. Note that the curve yields a value  $\lambda = -0.32$  at  $R_0 = 0$ , i.e. a decay rate of  $-0.32$  when the transmission is completely stopped. This exponent matches well with the final decay of newly confirmed cases in Fig. 2b.

## Serial interval

An important consistency check of our model assumptions is to carry out a comparison between the statistics of the symptom onset time of a given individual, and that of the symptom onset lag between primary and secondary infections, which is known as the serial interval. A large data set was compiled by Du et al.<sup>4</sup> that included 468 serial cases, from which the serial interval statistics can be extracted. In particular, the mean serial interval length is between 4 to 4.5 days while the standard deviation is around 4.8 days. In the Supplementary Information, we present an analysis of the statistics of the serial interval from our model. The mean value of the serial interval is predicted to be the same as that of the symptom onset time, while the standard deviation is  $\sqrt{3}$  times greater than that of the symptom onset time. Both numbers are about 10-20% larger than the observed values. The blue line in Fig. 3c shows the predicted serial interval distribution obtained from the symptom onset time distribution (black dots in a). Very good agreement between the two data sets from independent studies is seen. As noted by Du et al.<sup>4</sup>, the discontinuity across the origin may be attributed to the false assignment of infector and infectee in a pair. Cluster infections (such as intra-family transmission) could also yield a lower value for the serial interval on average, contributing to the discrepancy seen in the figure. Overall, the comparison lends strong support for the aggregated symptom onset time distribution obtained, as well as for our model assumptions.

## Interpretation of the three-phase epidemic growth and decay

To show that our model can be adapted to achieve a better understanding of the three phases of epidemic progression shown in Fig. 2, we have performed numerical simulations with a time-dependent transmission rate  $\beta(t)$ . For simplicity, the kernel function was chosen to correspond to the red line shown in Fig. 3a. The exit rates from the  $A$  state was set to  $\alpha_A = 2\gamma_A = 0.4$  /day. This choice limits the time window for pre-symptomatic transmission to less than 2 days on average.

### Import driven phase

Around the time of the Wuhan lockdown, there was a massive exit of about 5 million people from Hubei province that lasted for several days. This happened when the number of newly confirmed cases in Hubei province was still increasing. Therefore, the number of infected individuals traveling each day from Wuhan to other places also increased at the same rate. As travellers went separate ways, they act independently as assumed in our model, instead of forming large clusters. Data from the most affected provinces shows that the majority of confirmed cases in the first two weeks after the lockdown were either working in Wuhan or had recently traveled to the city<sup>34</sup>. Other than Hubei province, isolation and social-distancing measures were swiftly introduced, which essentially limited local outbreaks except in a few well-documented cases.

We model the growth of the infected population in provinces other than Hubei by adding a source term to Eq. (1) due to the imported cases prior to the lockdown, whose magnitude increases exponentially at a rate  $\lambda_0$ . As the lockdown occurred only a few days before the Chinese New Year, transportation around the country was working at full capacity. This makes it reasonable to assume a constant flux of people from Hubei province. We also assume the

local value of  $R_0$  to be somewhat smaller than its value in Hubei at the time due to the much greater capacity to track infected and suspected individuals. As we explain in the Supplementary Information, the growth rate of the infected population is then set by the  $\lambda_0$  for imported cases at a constant influx. The lockdown drastically decreased the number of new imports. Taking into account the incubation period, we allow the amplitude of the source term to decrease linearly to zero over a period of 10 days.

The red and blue lines in Fig. 4 show our numerical solutions with initially null infection. In the first day or two,  $A$  grows faster than  $\lambda_0$ , but approaches the exponential growth phase with a rate close to  $\lambda_0$  in subsequent days. Data from different provinces show a “universal” growth rate as they are all driven by the same pace-maker (Fig. 2a and 2b). Once infection from imported cases came to a halt (chosen to be 10 days in our simulation), the disease took its own course in the local community, at which point the epidemic development in different communities began to diverge, as we discuss next.

### Crossover behaviour due to changing social distancing measures

Upon instituting strict population mobility controls, such as closing borders, restricting travel, tracing close contacts and quarantining, the growth rate of newly confirmed cases will gradually transition from a constant positive value to lower values and eventually become negative.

Specifically, in our model framework, we consider a situation where a new social distancing policy is introduced on a certain date  $t_0$  such that

$$\beta(t) = \beta_0 \left(1 - \frac{t - t_0}{T}\right) + \beta_1 \left(\frac{t - t_0}{T}\right), \quad t_0 < t < t_0 + T$$

Here  $T$  is the time it takes for the full implementation of the policy. After this period,  $\beta(t) = \beta_1$ . In the extreme case,  $\beta_1 = 0$  which is used in our simulations. The equation for  $A$  is then modified to,

$$\dot{A} = -(\alpha_A + \gamma_A)A + \int_{-\infty}^t \beta_A(t_1) \alpha_E(t - t_1) q_E(t - t_1) A(t_1) dt_1 \quad (6)$$

To simulate the daily pattern of confirmed cases, we set  $t_0$  to be one week after the lockdown. The blue, red and black curves in Fig. 4 correspond to three different values of  $T$  given in the legend. Taken at face value, our model can reproduce fast or slow crossovers seen in the data from various provinces of China.

It is interesting to note that the reported data from individual provinces show universal and predictable behaviour when the majority of daily confirmed cases are imported from the most severely hit region. As border control and other measures are introduced, local infections eventually take over. The data then show large fluctuations due to cluster infection. Therefore dominance by imported or local cases can be readily distinguished on the plot when the total number of infected cases is on the order of a few hundred.

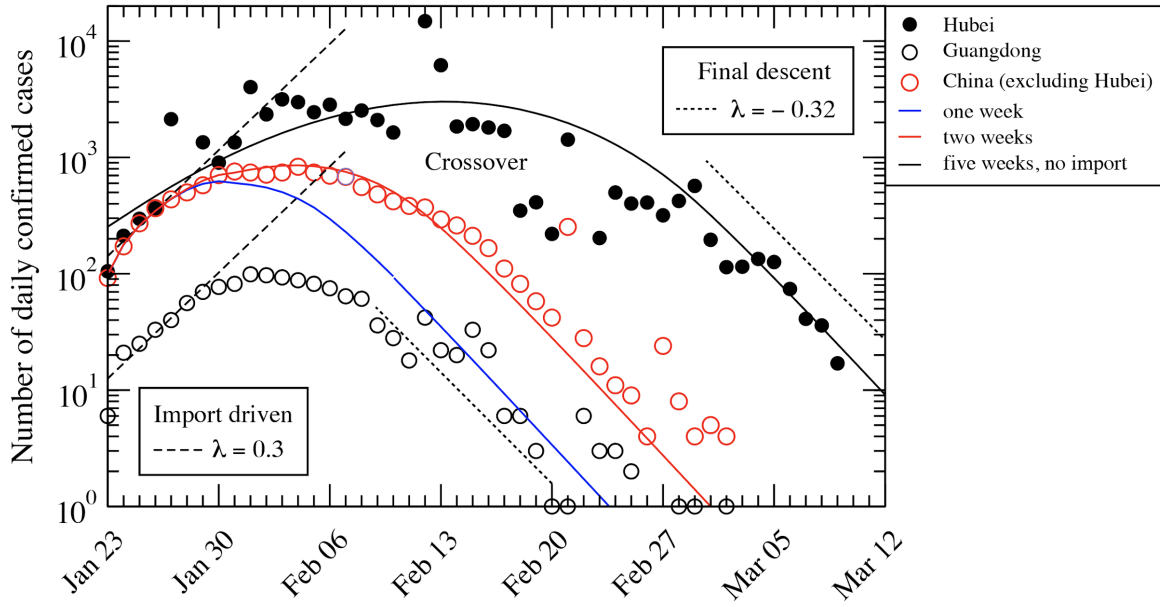


**Figure 4. The universal pattern of COVID-19 transmission predicted by the model.** Model-predicted evolution of the number of daily confirmed cases with a linear decay of infectiousness. Here, we assumed that the pre-symptomatic transmission rate will decrease linearly in a time window of one, two and five weeks, starting from one week after the Wuhan lockdown (day 0). This is intended to mimic the implementation of stringent control measures in different communities. The situation represented by blue and red curves is initially driven by imported cases whose number grows exponentially at a rate  $\lambda_0 = 0.2$  prior to the lockdown, with an amplitude that decreases linearly and vanishes on the 10th day after the lockdown. No imported cases were introduced to generate the black curve. The number of daily confirmed cases in Hubei, Guangdong and China (excluding Hubei) are replotted for comparison. Cluster infections result in occasional bursts in the time series which are not modelled in this work.

### Final decay

Once strict mobility restrictions and social distancing measures are taken, the model shows that new confirmed cases per day will go into an exponential decay phase. More importantly, the model gives the decay rate (Fig. 1a and 1b, dashed-black line in phase III,  $\lambda = -0.32$ ) to be exactly the same as the decay rate (Fig. 3a, dashed-black line,  $\lambda = -0.32$ ) of the tail of the incubation-period distribution. This is the upper bound of the decay rate, i.e., the fastest decay rate that we can achieve by isolating individuals without actively screening the whole population.

## Conclusion

We have constructed the first explicit model for the evolution of the pre-symptomatic COVID-19 population in the form of a delayed integro-differential equation whose kernel function can be obtained directly from the symptom onset time distribution. For a fixed disease transmission rate, the model yields exponentially growing or decaying solutions, where the growth rate  $\lambda$  is related to the basic reproduction number through the Laplace transform of the symptom onset

time distribution function. With this empirically-based but quantitative model, one can examine the effectiveness of various control measures on epidemic development over time. More interestingly, it also predicts an upper bound to how fast an epidemic can disappear as measured by a universal decay rate set by the tail of the symptom onset time distribution. In the case of the epidemic evolution of Hubei province, for example, this limiting decay rate was reached around March 3, 2020, offering vindication that the outbreak was finally brought under control.

While the outbreak is subsiding in China, it has escalated in multiple countries across the world, threatening a repeat of the Wuhan trauma. Asymptomatic transmission poses a major and ongoing challenge to disease control by national governments who do not have the option to impose strict human mobility measures as China did. As the epidemic center shifts to regions outside of China, the prevalence of import cases becomes much higher and more difficult to control. The quantitative equations presented in the Model section will help policymakers to design measures to decrease  $R_0$  given by Eq. (3), and to assess their effectiveness through continuous monitoring of the epidemic development, should the asymptomatic population be the dominating mode of COVID-19 transmission.

Early detection through screening of inbound travellers, testing in epidemic centers or clusters, and contact tracing from the date of suspected infection, would limit the growth of the pre-symptomatic group. More conservative quarantine measures, general social distancing and proactive hygiene practices are also crucial to reducing transmission. Finally, leadership and effective communication from global and national institutions are critical to coordinating resources and reassuring the public. Given adequate policy response, newly confirmed cases will inevitably begin a contracting course at a rate of  $-0.32$  per day, eventually leading to full containment of the current pandemic.

## Acknowledgments

The work is supported in part by the NSFC under Grant Nos. 11635002 and U1530402, and by the Research Grants Council of the Hong Kong Special Administrative Region (HKSAR) under Grant Nos. HKBU 12324716.

## Conflict of Interest Statement

Authors declare no conflict of interest.

## Disclaimer

Any views expressed by Jiang Liu and Viola Tang are not as a representative speaking for or on behalf of his/her employer, nor do they represent his/her employer's positions, strategies or opinions.

## References:

1. WHO. WHO Director-General's opening remarks at the mission briefing on COVID-19 - 26 February 2020. 1–6 (2020). Available at: <https://www.who.int/dg/speeches/detail/who-director-general-s-opening-remarks-at-the-media-briefing-on-covid-19---11-march-2020>. (Accessed: 13th March 2020)
2. Dong, E., Du, H. & Gardner, L. An interactive web-based dashboard to track COVID-19 in real time. *Lancet Infect. Dis.* **3099**, 19–20 (2020).
3. Tindale, L. *et al.* Transmission interval estimates suggest pre-symptomatic spread of COVID-19. *medRxiv* 2020.03.03.20029983 (2020). doi:10.1101/2020.03.03.20029983
4. Du, Z. *et al.* The serial interval of COVID-19 from publicly reported confirmed cases. *medRxiv* 2020.02.19.20025452 (2020). doi:10.1101/2020.02.19.20025452
5. Huang, R., Xia, J., Chen, Y., Shan, C. & Wu, C. A family cluster of SARS-CoV-2 infection involving 11 patients in Nanjing, China. *Lancet. Infect. Dis.* **0**, (2020).
6. Anderson, R. M., Heesterbeek, H., Klinkenberg, D. & Hollingsworth, T. D. How will country-based mitigation measures influence the course of the COVID-19 epidemic? *Lancet* **0**, (2020).
7. Hu, Z. Z. *et al.* Clinical characteristics of 24 asymptomatic infections with COVID-19 screened among close contacts in Nanjing, China. *Sci. China Life Sci.* 1–6 (2020). doi:10.1007/s11427-020-1661-4
8. Zhou, P. *et al.* A pneumonia outbreak associated with a new coronavirus of probable bat origin. *Nature* (2020). doi:10.1038/s41586-020-2012-7
9. Wu, F. *et al.* A new coronavirus associated with human respiratory disease in China. *Nature* (2020). doi:10.1038/s41586-020-2008-3
10. Li, Q. *et al.* Early Transmission Dynamics in Wuhan, China, of Novel Coronavirus-Infected Pneumonia. *N. Engl. J. Med.* (2020). doi:10.1056/nejmoa2001316
11. Bai, Y. *et al.* Presumed Asymptomatic Carrier Transmission of COVID-19. *JAMA* (2020). doi:10.1001/jama.2020.2565
12. National Institute of Infectious Diseases Japan. Field Briefing: Diamond Princess COVID-19 Cases. (2020). Available at: <https://www.niid.go.jp/niid/en/2019-ncov-e/9417-covid-dp-fe-02.html>. (Accessed: 15th March 2020)
13. Mizumoto, K., Kagaya, K., Zarebski, A. & Chowell, G. Estimating the Asymptomatic Proportion of 2019 Novel Coronavirus onboard the Princess Cruises Ship, 2020. *medRxiv* 2020.02.20.20025866 (2020). doi:10.1101/2020.02.20.20025866
14. Nishiura, H., Linton, N. M. & Akhmetzhanov, A. R. Serial interval of novel coronavirus (COVID-19) infections. *Int. J. Infect. Dis.* (2020). doi:10.1016/j.ijid.2020.02.060
15. Xia, W. *et al.* Transmission of corona virus disease 2019 during the incubation period may lead to a quarantine loophole. *medRxiv* 2020.03.06.20031955 (2020). doi:10.1101/2020.03.06.20031955
16. Zhao, S. *et al.* Estimating the serial interval of the novel coronavirus disease (COVID-19): A statistical analysis using the public data in Hong Kong from January 16 to February 15, 2020. *medRxiv* 2020.02.21.20026559 (2020). doi:10.1101/2020.02.21.20026559
17. Zhao, S. *et al.* Preliminary estimation of the basic reproduction number of novel coronavirus (2019-nCoV) in China, from 2019 to 2020: A data-driven analysis in the early phase of the outbreak. *Int. J. Infect. Dis.* **92**, 214–217 (2020).

18. You, C. *et al.* Estimation of the Time-Varying Reproduction Number of COVID-19 Outbreak in China. *medRxiv* 2020.02.08.20021253 (2020). doi:10.1101/2020.02.08.20021253
19. Zhang, S. *et al.* Estimation of the reproductive number of Novel Coronavirus (COVID-19) and the probable outbreak size on the Diamond Princess cruise ship: A data-driven analysis. *Int. J. Infect. Dis.* **93**, 201–204 (2020).
20. Wang, Y. *et al.* Estimating the basic reproduction number of COVID-19 in Wuhan, China. *Chinese J. Epidemiol.* **41**, 476–479 (2020).
21. Tang, B. *et al.* The evolution of quarantined and suspected cases determines the final trend of the 2019-nCoV epidemics based on multi-source data analyses. *SSRN eLibrary* (2020).
22. Mizumoto, K. & Chowell, G. Transmission potential of the New Corona (COVID-19) onboard the Princess Cruises Ship, 2020. *Infect. Dis. Model.* **5**, 264–270 (2020).
23. Read, J. M., Bridgen, J. R., Cummings, D. A., Ho, A. & Jewell, C. P. Novel coronavirus 2019-nCoV: early estimation of epidemiological parameters and epidemic predictions. *medRxiv* **2020**, 2020.01.23.20018549 (2020).
24. Hermanowicz, S. W. Forecasting the Wuhan coronavirus (2019-nCoV) epidemics using a simple (simplistic) model. *medRxiv* 2020.02.04.20020461 (2020). doi:10.1101/2020.02.04.20020461
25. Wallinga, J. & Lipsitch, M. How generation intervals shape the relationship between growth rates and reproductive numbers. *Proc. R. Soc. B Biol. Sci.* **274**, 599–604 (2007).
26. Hellewell, J. *et al.* Feasibility of controlling COVID-19 outbreaks by isolation of cases and contacts. *Lancet. Glob. Heal.* **0**, (2020).
27. Pan, J. *et al.* Effectiveness of control strategies for Coronavirus Disease 2019: a SEIR dynamic modeling study. *medRxiv* 2020.02.19.20025387 (2020). doi:10.1101/2020.02.19.20025387
28. Zu, J. *et al.* Epidemic Trend and Transmission Risk of SARS-CoV-2 after Government Intervention in the Mainland of China: A Mathematical Model Study. *Lancet* (2020).
29. Fraser, C., Riley, S., Anderson, R. M. & Ferguson, N. M. Factors that make an infectious disease outbreak controllable. *Proc. Natl. Acad. Sci. U. S. A.* **101**, 6146–51 (2004).
30. Grassly, N. C. & Fraser, C. Mathematical models of infectious disease transmission. *Nature Reviews Microbiology* **6**, 477–487 (2008).
31. Lu, H. *et al.* A descriptive study of the impact of diseases control and prevention on the epidemics dynamics and clinical features of SARS-CoV-2 outbreak in Shanghai, lessons learned for metropolis epidemics prevention. *medRxiv* 2020.02.19.20025031 (2020). doi:10.1101/2020.02.19.20025031
32. Men, K. *et al.* Estimate the incubation period of coronavirus 2019 (COVID-19). *medRxiv* 2020.02.24.20027474 (2020). doi:10.1101/2020.02.24.20027474
33. Murray, J. D. *Mathematical Biology I. An introduction. Interdisciplinary Applied Mathematics* (2002). doi:10.1007/b98868
34. Epidemiology Working Group for NCIP Epidemic Response. The epidemiological characteristics of an outbreak of 2019 novel coronavirus diseases (COVID-19) in China. *Chinese J. Epidemiol.* **41**, 145–151 (2020).

## Supplementary Information

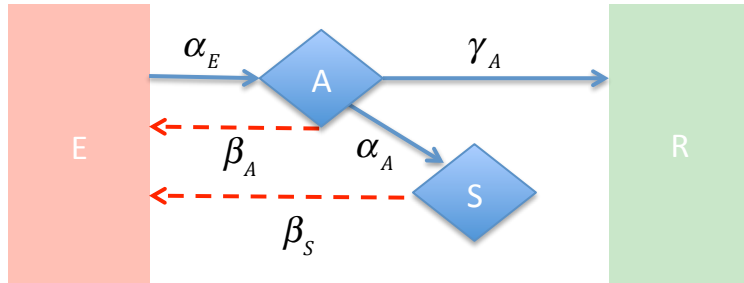
### Pre-symptomatic Transmission in the Evolution of the COVID-19 Pandemic

In this Supplementary Information, detailed information about our linear model of asymptomatic carriers with delay kernels for incubation and infection is listed.

A prominent feature of the COVID-19 outbreak is transmission by asymptomatic carriers ( $A$ ) of the SARS-CoV-2 virus. Quantitative understanding of the time evolution of the  $A$  population in specific communities is crucial for the design and assessment of various quarantine measures.

#### Model

The basic structure of the model introduced in the Main Text, illustrated by the diagram below for easy reference. To better account for observational data, we take  $\alpha_E$  and  $\beta_S$  to be functions of the time an individual is in state  $E$  (exposed) and state  $S$  (symptomatic) since respective onsets. The other parameters are treated as constants for a given community.



Let's consider first the generation rate of  $E$  at time  $t$ :

$$J_E(t) = \beta_A A(t) + \int_{-\infty}^t \beta_S(t-t_2) dS(t_2)$$

These “newly exposed” eventually make their way to  $A$ . The flux to  $A$  due to a group exposed at a time  $t_1 < t$  is given by,

$$dJ_A(t) = \alpha_E(t-t_1) q_E(t-t_1) J_E(t_1) dt_1$$

$$q_E(t) = e^{-\int_0^t \alpha_E(t_1) dt_1}$$

Adding up contributions from all such groups, we obtain

$$J_A(t) = \int_{-\infty}^t \alpha_E(t-t_1) q_E(t-t_1) J_E(t_1) dt_1$$

Note that in our model,  $dS(t) = \alpha_A A(t) dt$ , we have then

$$J_A(t) = \int_{-\infty}^t \beta_A \alpha_E(t-t_1) q_E(t-t_1) A(t_1) dt_1 + \int_{-\infty}^t \alpha_E(t-t_1) q_E(t-t_1) dt_1 \int_{-\infty}^{t_1} \beta_S(t_1-t_2) \alpha_A A(t_2) dt_2$$

$$= \int_{-\infty}^t K(t-t_1, t_1) A(t_1) dt_1$$

Here the kernel function is given by,

$$K(t) = \beta_A \alpha_E(t) q_E(t) + \alpha_A \int_0^t \alpha_E(t-t_1) q_E(t-t_1) \beta_S(t_1) dt_1 \quad (\text{S1})$$

The final equation for A takes the form,

$$\dot{A} = -(\alpha_A + \gamma_A) A + \int_{-\infty}^t K(t-t_1) A(t_1) dt_1 \quad (\text{S2})$$

### **Kernel function from observed symptom onset time distribution**

As we show below, a major advantage of our model is that the kernel function in Eq. (S2) can be determined from the statistics of the time interval between exposure and symptom onset  $\tau_o = \tau_E + \tau_A$ , directly observable from clinical case studies. In the second phase of this interval (i.e., A), the individual is infectious. Assuming the two dwell times to be statistically independent, we have the convolution formula,

$$\text{Prob}(\tau_o > t) \equiv \int_t^\infty dt_1 p_o(t_1) = \text{Prob}(\tau_E + \tau_A > t) = \int_t^\infty dt_1 p_A(t_1) + \int_0^t dt_1 p_A(t_1) q_E(t-t_1)$$

Here  $p_A(t) = \alpha_A e^{-\alpha_A t}$  denotes distribute of the dwell time  $\tau_A$  in state A before symptom onset. In terms of Laplace transform, we have

$$\frac{1 - \tilde{p}_o(\lambda)}{\lambda} = \frac{1}{\alpha_A + \lambda} + \frac{\alpha_A}{\alpha_A + \lambda} \tilde{q}_E(\lambda)$$

from which we obtain,

$$\tilde{q}_E(\lambda) = \left( \frac{1}{\lambda} + \frac{1}{\alpha_A} \right) \left[ 1 - \tilde{p}_o(\lambda) \right] - \frac{1}{\alpha_A} \quad (\text{S3})$$

The Laplace transform of Eq. (S1) yields

$$\tilde{K}(\lambda) \equiv \int_0^\infty K(t) e^{-\lambda t} dt = \left[ \beta_A + \alpha_A \tilde{\beta}_S(\lambda) \right] \left[ 1 - \lambda \tilde{q}_E(\lambda) \right] \quad (\text{S4})$$

With the help of (S3), we have finally

$$\tilde{K}(\lambda) = \left[ \beta_A + \alpha_A \tilde{\beta}_S(\lambda) \right] \left( 1 + \frac{\lambda}{\alpha_A} \right) \tilde{p}_o(\lambda) \quad (\text{S5})$$

When the public health and medical resources are not overstretched, patients showing symptoms of COVID-19 can soon be identified and isolated. This restricts symptomatic transmission to the first couple of days of symptom onset. In such a scenario, we may write  $\beta_S(t) = \tilde{\beta}_S \delta(t)$ , where  $\delta(t)$  is the Dirac delta function.

Consequently,  $\tilde{\beta}_S(\lambda) = \tilde{\beta}_S$  is a constant. Carrying out inverse Laplace transform of (S5), we obtain,

$$K(t) = \frac{\beta_A + \alpha_A \tilde{\beta}_S}{\alpha_A} \left[ \alpha_A p_o(t) + \frac{d}{dt} p_o(t) \right] \quad (\text{S6})$$

## Exponential growth/decay

Let's seek an exponential growth solution to equation (S2),

$$A(t) = e^{\lambda t}$$

Substituting into the above equation, we obtain the eigenvalue equation,

$$\lambda = -(\alpha_A + \gamma_A) + \tilde{K}(\lambda) \quad (\text{S7})$$

Solution of Eq. (S7) yields the rate of the exponential growth (or decay) of the infected population.

## $R_0$

$R_0$  is defined to be the number of secondary  $A$ 's generated by a given  $A$ . This number has two contributions, i.e., when  $A$  remains in state  $A$  and after  $A$  changes to  $S$ .

Adding up the two yields,

$$R_0 = \int_0^\infty \beta_A t e^{-(\alpha_A + \gamma_A)t} (\alpha_A + \gamma_A) dt + \frac{\alpha_A}{\alpha_A + \gamma_A} \int_0^\infty \beta_S(t) dt = \frac{\beta_A + \alpha_A \tilde{\beta}_S(0)}{\alpha_A + \gamma_A} \quad (\text{S8})$$

From Eq. (S7), we see that the condition for  $\lambda = 0$  is

$$\tilde{K}(0) = \alpha_A + \gamma_A = \beta_A + \alpha_A \tilde{\beta}_S(0)$$

which is precisely the condition  $R_0 = 1$ !

Combining Eq. (S5) with Eq. (S7), we obtain,

$$[\beta_A + \alpha_A \tilde{\beta}_S(\lambda)] \left( 1 + \frac{\lambda}{\alpha_A} \right) \tilde{p}_o(\lambda) = \lambda + \alpha_A + \gamma_A$$

or

$$[\beta_A + \alpha_A \tilde{\beta}_S(\lambda)] \tilde{p}_o(\lambda) = \alpha_A \left( 1 + \frac{\gamma_A}{\lambda + \alpha_A} \right) \quad (\text{S9})$$

For short infectious duration of symptomatic patients, we may approximate  $\tilde{\beta}(\lambda) \approx \tilde{\beta}(0)$  and rewrite Eq. (S9) as

$$R_0 \approx \frac{1}{\tilde{p}_o(\lambda)} \left( 1 - \frac{\lambda}{\lambda + \alpha_A} \frac{\gamma_A}{\gamma_A + \alpha_A} \right) \quad (\text{S10})$$

Walling and Lipsitch [2] proposed an equation for  $R_0$  which resembles (S10). Their result is a mathematical identity based on the mean reproductive rate  $r(t)$  of an individual who is newly exposed at  $t = 0$ . In our current setting,

$$\begin{aligned} r(t) &= \beta_A \int_0^t q_E(t_1) \alpha_E(t_1) dt_1 e^{-(\alpha_A + \gamma_A)(t-t_1)} + \int_0^t q_E(t_1) \alpha_E(t_1) dt_1 \int_{t_1}^t \beta_S(t-t_2) \alpha_A dt_2 e^{-(\alpha_A + \gamma_A)(t_2-t_1)} \\ &= \int_0^t dt_1 K(t_1) e^{-(\alpha_A + \gamma_A)(t-t_1)} \end{aligned}$$

where the last step is written by comparing with the expression for  $J_A(t)$ .

Now,

$$\tilde{r}(\lambda) = \frac{\tilde{K}(\lambda)}{\alpha_A + \gamma_A + \lambda} = \frac{\beta_A + \alpha_A \tilde{\beta}_S(\lambda)}{\alpha_A + \gamma_A + \lambda} \left(1 + \frac{\lambda}{\alpha_A}\right) \tilde{p}_o(\lambda) \quad (\text{S11})$$

Walling and Lipsitch [1] introduced the normalization constant

$$R_0 = \int_0^\infty r(t) dt = \tilde{r}(0) = \frac{\beta_A + \alpha_A \tilde{\beta}_S(0)}{\alpha_A + \gamma_A}$$

which agrees with Eq. (S8). They defined a quantity  $g(t) = r(t)/R_0$  as the normalized “generation interval distribution”. Consequently, at the observed population growth rate  $\lambda$ ,

$$\tilde{g}(\lambda) = \frac{\tilde{r}(\lambda)}{R_0} = \frac{1}{R_0},$$

known as the Lotka–Euler estimating equation. This equation is equivalent to (S10).

### A Markovian model

A number of modeling studies in the literature adopt a Markovian set up with  $\alpha_E(t) = \text{const}$ , which can be considered as a special case of our kernel function approach. In particular,

$$\tilde{q}_E = \frac{1}{\alpha_E + \lambda}, \quad \tilde{p}_o = \frac{\alpha_E}{\alpha_E + \lambda} \frac{\alpha_A}{\alpha_A + \lambda}$$

The Laplace transform of the kernel function then takes the form,

$$\tilde{K}_M(\lambda) = \alpha_E \frac{\beta_A + \alpha_A \tilde{\beta}_S(\lambda)}{\alpha_E + \lambda} \approx \alpha_E \frac{\beta_A + \alpha_A \tilde{\beta}_S}{\alpha_E + \lambda} \quad (\text{S12})$$

Performing inverse transform yields

$$K_M(t) = \beta_A \alpha_E e^{-\alpha_E t} + \alpha_A \alpha_E \int_0^t e^{-\alpha_E(t-t_1)} \beta_S(t_1) dt_1 \approx (\beta_A + \alpha_A \tilde{\beta}_S) \alpha_E e^{-\alpha_E t} \quad (\text{S13})$$

Let  $\tau_o = \alpha_E^{-1} + \alpha_A^{-1}$ ,  $\varepsilon = \frac{\alpha_A}{\alpha_E + \alpha_A}$ , we have from Eq. (S10),

$$R_0 \approx \left(1 + \frac{\lambda}{\alpha_E}\right) \left(1 + \frac{\lambda}{\alpha_A + \gamma_A}\right),$$

i.e., a parabola with two nodes at  $\lambda_E = -\alpha_E$  and  $\lambda_A = -\alpha_A - \gamma_A$ . In this case, the epidemic decay rate is set by the smaller of the two: the rate of transition from exposed to infectious, and the rate of removal of the asymptomatic infectors.

Solving the quadratic equation yields,

$$\lambda = \frac{1}{\tau_o} \frac{2(R_0 - 1)}{1 + \sqrt{1 + 4\epsilon(1-\epsilon)(R_0 - 1)}}$$

The onset time distribution in this case is given by

$$p_o(t) = \frac{\alpha_E \alpha_A}{\alpha_A - \alpha_E} \left[ e^{-\alpha_E t} - e^{-\alpha_A t} \right] = \frac{1}{\tau_E - \tau_A} \left( e^{-t/\tau_E} - e^{-t/\tau_A} \right)$$

with its mean and variance given by,

$$\tau_o = \langle t_o \rangle = \tau_E + \tau_A, \quad \sigma_o^2 = \langle t_o^2 \rangle - \langle t_o \rangle^2 = \tau_E^2 + \tau_A^2, \quad \frac{\sigma_o^2}{\tau_o^2} = \epsilon^2 + (1-\epsilon)^2$$

where  $\tau_E = \epsilon \tau_o$ ,  $\tau_A = (1-\epsilon) \tau_o$ . In the limit  $\tau_E = \tau_A$  or  $\epsilon = 1/2$ ,  $p_o(t) = \frac{t}{\tau_E^2} e^{-t/\tau_E}$ .

### **Symptom onset time distribution from case studies**

Based on previous studies, the actual symptom onset time distribution are illustrated in the Fig.3(a) of the main text. The tail of the distribution is well fitted by an exponential function with a decay rate of 0.32/day (dashed line). The red curve gives prediction of the Markov model at  $\epsilon = 1/2$  and  $\tau_E = \tau_o/2 = 2.75$ ,  $\alpha_E = \tau_E^{-1} = 0.36$ .

Note that this choice yields the minimum ratio for  $\sigma_o/\tau_o = 1/\sqrt{2}$  which is still greater than the value 0.56 from the data. The peak of the distribution from the Markov model is at a shorter time as compared to the actual data. This suggests a more general  $\alpha_E(t)$  is to be used. The issue should be revisited as more data become available in the future.

### **Serial interval statistics**

Previous study [2] reported the statistics of the time lag in symptom onset between infector–infectee pairs in 468 confirmed serial infection cases.

Let  $t = 0$  be the time point when the infector X is exposed to the virus, the distribution of the transmission time  $t_{X \rightarrow Y}$  from X to Y is  $g(t)$ .

We now consider the distribution of the difference in symptom onset time  $t_{XY} = t_Y - t_X$  between X and Y. The distribution of  $t_X$  is given by  $p_o(t)$ . The distribution of  $t_Y = t_{X \rightarrow Y} + t_Y'$  can also be expressed as a convolution of  $g(t)$  and  $p_o(t)$ . In the absence of the inactivation process (i.e.,  $\gamma_A = 0$ ),  $g(t) \approx p_o(t)$ , all three quantities have the same distribution. Consequently,  $\sigma_X = \frac{\sigma_{XY}}{\sqrt{3}}$ .

From the Table S1 of Ref [2], we get SD values 2.74, broadly consistent with the value 3.1 from our analysis. They also reported a mean serial interval of 3.96 days, but a longer period of 4.56 days for non-household secondary transmission. Both are shorter than the mean time of 5.5 days for symptom onset. We are in the process of

investigating the cause of the small but systematic discrepancy between the serial infection data and our model predictions.

### Solution with imported cases

Growth driven by imported cases can be modeled by adding a source term to Eq. (S2),

$$\dot{A} = -(\alpha_A + \gamma_A)A + \int_{-\infty}^t K(t-t_1)A(t_1)dt_1 + S(t) \quad (\text{S14})$$

Consider a simple case where the imported cases grow exponentially with a rate  $\lambda_I$ , i.e.,  $S(t) = S_I e^{\lambda_I t}$ . Let's first seek an exponentially growing solution where the local population is driven by the imported cases,

$$\begin{aligned} A(t) &= A_{\text{all}} e^{\lambda_I t} \\ (\lambda_I + \alpha_A + \gamma_A)A_{\text{all}} &= A_{\text{all}} \tilde{K}(\lambda_I) + S_I \\ A_{\text{all}} &= \frac{S_I}{\lambda_I + \alpha_A + \gamma_A - \tilde{K}(\lambda_I)} \end{aligned}$$

The fraction of local infection cases after the initial transient is given by,

$$\frac{A_{\text{local}}}{A_{\text{all}}} = \frac{\tilde{K}(\lambda_I)}{\lambda_I + \alpha_A + \gamma_A}$$

We now derive a complete solution using the simplified kernel (S12), starting from the date of massive import. The local infection at  $t = 0$  is assumed to be zero. Laplace transform of the equation yields

$$\begin{aligned} \lambda \tilde{A}(\lambda) &= -(\alpha_A + \gamma_A) \tilde{A}(\lambda) + \tilde{K}(\lambda) \tilde{A}(\lambda) + \tilde{S}(\lambda) \\ \tilde{A}(\lambda) &= \frac{\tilde{S}(\lambda)}{\alpha_A + \gamma_A + \lambda - \tilde{K}(\lambda)} \end{aligned}$$

$$\begin{aligned} \tilde{A}(\lambda) &= \frac{1}{\alpha_A + \gamma_A + \lambda - R_0(\alpha_A + \gamma_A) \frac{\alpha_E}{\lambda + \alpha_E}} \frac{S_I}{\lambda - \lambda_I} \\ &= \frac{\lambda + \alpha_E}{\lambda^2 + (\alpha_E + \alpha_A + \gamma_A)\lambda - (R_0 - 1)\alpha_E(\alpha_A + \gamma_A)} \frac{S_I}{\lambda - \lambda_I} \end{aligned}$$

Routes of the quadratic equation

$$\lambda^2 + (\alpha_E + \alpha_A + \gamma_A)\lambda - (R_0 - 1)\alpha_E(\alpha_A + \gamma_A) = 0$$

are given by,

$$\lambda_{\pm} = \frac{-(\alpha_E + \alpha_A + \gamma_A) \pm \sqrt{(\alpha_E + \alpha_A + \gamma_A)^2 + 4(R_0 - 1)\alpha_E(\alpha_A + \gamma_A)}}{2}$$

$$\begin{aligned}
\frac{\tilde{A}(\lambda)}{S_I} &= \frac{\lambda + \alpha_E}{(\lambda - \lambda_+)(\lambda - \lambda_-)(\lambda - \lambda_I)} = \frac{A_+}{\lambda - \lambda_+} + \frac{A_-}{\lambda - \lambda_-} + \frac{A_I}{\lambda - \lambda_I} \\
\lambda + \alpha_E &= A_+(\lambda - \lambda_-)(\lambda - \lambda_I) + A_-(\lambda - \lambda_+)(\lambda - \lambda_I) + A_I(\lambda - \lambda_+)(\lambda - \lambda_-) \\
A_+ &= \frac{\lambda_+ + \alpha_E}{(\lambda_+ - \lambda_-)(\lambda_+ - \lambda_I)} \\
A_- &= -\frac{\lambda_- + \alpha_E}{(\lambda_+ - \lambda_-)(\lambda_- - \lambda_I)} \\
A_I &= \frac{\lambda_I + \alpha_E}{(\lambda_I - \lambda_+)(\lambda_I - \lambda_-)}
\end{aligned}$$

The final solution is given by,

$$A(t) = S_I (A_+ e^{\lambda_+ t} + A_- e^{\lambda_- t} + A_I e^{\lambda_I t})$$

In the case of zero local transmission ( $R_0 = 0$ ), we have

$$A(t) = \frac{S_I}{\alpha_A + \gamma_A + \lambda_I} (e^{\lambda_I t} - e^{-(\alpha_A + \gamma_A)t})$$

This represents the minimal growth under a constant influx of people from infected region.

### **Crossover behaviour due to new social-distancing policy**

We now consider a situation when a new social-distancing policy is introduced on a certain date  $t_0$  such that

$$\beta_A(t) = \begin{cases} \beta_{A0}, & t < t_0 \\ \beta_{A1}, & t > t_0 \end{cases}.$$

As before, we shall set  $\beta_S(t) = \tilde{\beta}_S(0)\delta(t)$  so that its effect can be incorporated into an effective  $\beta_A$ . The equation for A is then modified to,

$$\dot{A} = -(\alpha_A + \gamma_A)A + \int_{-\infty}^t \beta_A(t_1) \alpha_E(t - t_1) q_E(t - t_1) A(t_1) dt_1 \quad (\text{S15})$$

For simplicity, we shall focus on the case of crossover between two exponential solutions set by the two  $\beta$ 's.

Without loss of generality, we may define our time such that  $t_0 = 0$ . Take

$A(t) = A_0 e^{\lambda_0 t}$  for  $t < t_0 = 0$ , we may rewrite the above equation as,

$$\dot{A} = -(\alpha_A + \gamma_A)A + \beta_{A0} \int_{-\infty}^0 \alpha_E(t - t_1) q_E(t - t_1) A_0 e^{\lambda_0 t_1} dt_1 + \beta_{A1} \int_0^t \alpha_E(t - t_1) q_E(t - t_1) A(t_1) dt_1$$

This is similar to our previous problem with a different source term. Again, by applying Laplace transform, we have,

$$\begin{aligned}
-A_0 + \lambda \tilde{A}(\lambda) &= -(\alpha_A + \gamma_A) \tilde{A}(\lambda) + \tilde{K}_1(\lambda) \tilde{A}(\lambda) + \tilde{S}(\lambda) \\
\tilde{A}(\lambda) &= \frac{\tilde{S}(\lambda) + A_0}{\alpha_A + \gamma_A + \lambda - \tilde{K}_1(\lambda)}
\end{aligned}$$

Here

$$\begin{aligned}
S(t) &= \beta_{A0} A_0 \int_{-\infty}^0 \alpha_E(t-t_1) q_E(t-t_1) e^{\lambda_0 t_1} dt_1 \\
&= \beta_{A0} A_0 \int_{-\infty}^t \alpha_E(t-t_1) q_E(t-t_1) e^{\lambda_0 t_1} dt_1 - \beta_{A0} A_0 \int_0^t \alpha_E(t-t_1) q_E(t-t_1) e^{\lambda_0 t_1} dt_1 \\
\tilde{S}(\lambda) &= \beta_{A0} A_0 \frac{\widetilde{\alpha_E q_E}(\lambda_0) - \widetilde{\alpha_E q_E}(\lambda_0)}{\lambda - \lambda_0} = \beta_{A0} A_0 \frac{\lambda \tilde{q}_E(\lambda) - \lambda_0 \tilde{q}_E(\lambda_0)}{\lambda - \lambda_0}
\end{aligned}$$

Simplified kernel:  $\tilde{q}_E(\lambda) = \frac{1}{\alpha_E + \lambda}$

$$\begin{aligned}
\tilde{S}(\lambda) &= \beta_{A0} A_0 \frac{\lambda(\alpha_E + \lambda_0) - \lambda_0(\alpha_E + \lambda)}{\lambda - \lambda_0} \frac{1}{(\alpha_E + \lambda_0)(\alpha_E + \lambda)} \\
&= \frac{\alpha_E \beta_{A0} A_0}{\alpha_E + \lambda_0} \frac{1}{\alpha_E + \lambda}
\end{aligned}$$

Compared to the solution in the imported case, all we need to do is to perform the substitution

$$S_I \rightarrow \frac{\alpha_E \beta_{A0}}{\alpha_E + \lambda_0} A_0 = \tilde{K}(\lambda_0) A_0 = (\lambda_0 + \alpha_A + \gamma_A) A_0, \quad \lambda_I \rightarrow -\alpha_E$$

In addition,  $A(0) = A_0$  gives an additional term, so that

$$\begin{aligned}
A(t) &= (\lambda_0 + \alpha_A + \gamma_A) A_0 \left( A_+ e^{\lambda_+ t} + A_- e^{\lambda_- t} + A_I e^{-\alpha_E t} \right) + A_0 \left( B_+ e^{\lambda_+ t} + B_- e^{\lambda_- t} \right) \\
B_+ &= \frac{\lambda_+ + \alpha_E}{\lambda_+ - \lambda_-}, \quad B_- = -\frac{\lambda_- + \alpha_E}{\lambda_+ - \lambda_-}
\end{aligned}$$

## References

[1] Wallinga, J., Lipsitch, M. How generation intervals shape the relationship between growth rates and reproductive numbers. Proc. R. Soc. B Biol. Sci. 274, 599–604 (2007).

[2] Du, Z. et al. The serial interval of COVID-19 from publicly reported confirmed cases. medRxiv 2020.02.19.20025452 (2020). doi:10.1101/2020.02.19.20025452.